

Clinical exome sequencing reveals locus heterogeneity and phenotypic variability of cohesinopathies

Bo Yuan, PhD^{1,2}, Juanita Neira, MD^{1,3}, Davut Pehlivan, MD^{1,4}, Teresa Santiago-Sim, PhD^{1,2}, Xiaofei Song, BS¹, Jill Rosenfeld, MS^{1,2}, Jennifer E. Posey, MD, PhD¹, Vipulkumar Patel, MS², Weihong Jin, MS², Margaret P. Adam, MD^{5,6}, Emma L. Baple, MBBS, PhD^{7,8}, John Dean, FRCP⁹, Chin-To Fong, MD¹⁰, Scott E. Hickey, MD¹¹, Louanne Hudgins, MD¹², Eyby Leon, MD¹³, Suneeta Madan-Khetarpal, MD¹⁴, Lettie Rawlins, MBChB^{7,8}, Cecilie F. Rustad, MD¹⁵, Asbjørg Stray-Pedersen, MD, PhD¹⁶, Kristian Tveten, PhD¹⁷, Olivia Wenger, MD¹⁸, Jullianne Diaz, MS¹³, Laura Jenkins, MS¹⁴, Laura Martin, MS¹⁰, Marianne McGuire, MS^{1,2}, Marguerite Pietryga, MS^{1,1}, Linda Ramsdell, MS^{5,6}, Leah Slattery, MS¹² DDD Study, Farida Abid, MD^{1,3,4}, Alison A. Bertuch, MD, PhD^{1,3}, Dorothy Grange, MD¹⁹, LaDonna Immken, MD²⁰, Christian P. Schaaf, MD, PhD^{1,3,21,22,23}, Hilde Van Esch, MD, PhD²⁴, Weimin Bi, PhD^{1,2}, Sau Wai Cheung, PhD, MBA^{1,2}, Amy M. Breman, PhD^{1,2}, Janice L. Smith, PhD^{1,2}, Chad Shaw, PhD^{1,2}, Andrew H. Crosby, PhD⁷, Christine Eng, MD^{1,2}, Yaping Yang, PhD^{1,2}, James R. Lupski, MD, PhD^{1,3,25}, Rui Xiao, PhD^{1,2} and Pengfei Liu, PhD^{1,2}

Purpose: Defects in the cohesin pathway are associated with cohesinopathies, notably Cornelia de Lange syndrome (CdLS). We aimed to delineate pathogenic variants in known and candidate cohesinopathy genes from a clinical exome perspective.

Methods: We retrospectively studied patients referred for clinical exome sequencing (CES, $N=10,698$). Patients with causative variants in novel or recently described cohesinopathy genes were enrolled for phenotypic characterization.

Results: Pathogenic or likely pathogenic single-nucleotide and insertion/deletion variants (SNVs/indels) were identified in established disease genes including *NIPBL* ($N=5$), *SMC1A* ($N=14$), *SMC3* ($N=4$), *RAD21* ($N=2$), and *HDAC8* ($N=8$). The phenotypes in this genetically defined cohort skew towards the mild end of CdLS spectrum as compared with phenotype-driven cohorts. Candidate or recently reported cohesinopathy genes were supported by de novo SNVs/indels in *STAG1* ($N=3$), *STAG2* ($N=$

5), *PDS5A* ($N=1$), and *WAPL* ($N=1$), and one inherited SNV in *PDS5A*. We also identified copy-number deletions affecting *STAG1* (two de novo, one of unknown inheritance) and *STAG2* (one of unknown inheritance). Patients with *STAG1* and *STAG2* variants presented with overlapping features yet without characteristic facial features of CdLS.

Conclusion: CES effectively identified disease-causing alleles at the mild end of the cohesinopathy spectrum and enabled characterization of candidate disease genes.

Genetics in Medicine (2019) 21:663–675; <https://doi.org/10.1038/s41436-018-0085-6>

Keywords: Atypical cohesinopathies; Clinical exome sequencing (CES); Cohesin pathway; *STAG1*; *STAG2*

INTRODUCTION

The cohesin complex mediates sister chromatid cohesion and ensures accurate chromosome segregation, recombination-mediated DNA repair, and genomic stability during DNA replication and cell division. Accumulating evidence suggests that cohesin is also involved in regulating chromosomal looping/architecture and gene transcriptional regulation.^{1–3}

Cohesin is a multisubunit protein complex composed of evolutionarily conserved core components encoded by

SMC1A (MIM *300040), *SMC3* (MIM *606062), *RAD21* (MIM *606462) and either *STAG1* (MIM *604358) or *STAG2* (MIM *300826) depending on the chromosomal location. Direct interaction between *SMC1A*, *SMC3*, and *RAD21* forms a tripartite ring structure that is used to entrap the replicated chromatin during sister chromatid cohesion (Fig. 1a). *STAG1/2* are the core structural component of functional cohesin and critical for the loading of cohesin onto chromatin during mitosis.^{1,2}

Correspondence: Pengfei Liu (pengfei.liu@bcm.edu). *Affiliations are listed at the end of the paper.

Submitted 23 December 2017; accepted: 1 June 2018

Published online: 30 August 2018

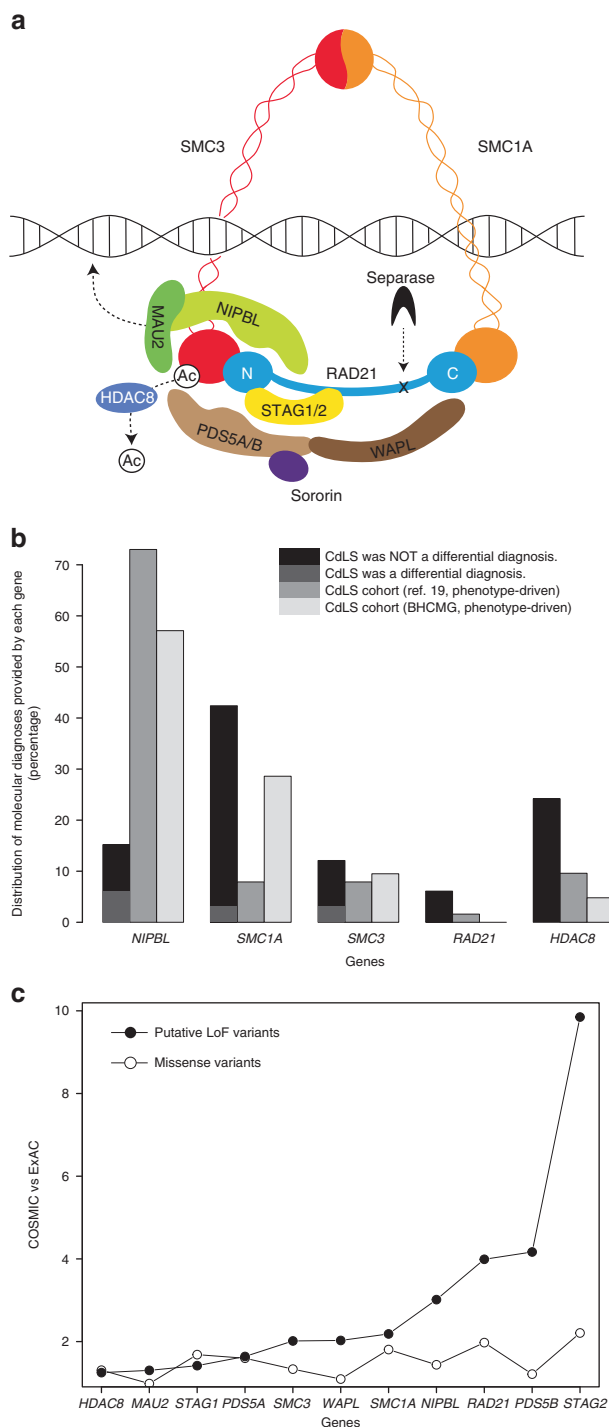


Fig. 1 Cohesin complex and its underlying genetic variants. **a** Schematic diagram of the cohesin complex. The components are represented in different color shapes labeled with protein names. **b** Comparison of genic distributions between our clinical exome cohort and two phenotype-driven cohorts of clinically diagnosed Cornelia de Lange syndrome (CdLS) patients (from ref. 19 and Baylor-Hopkins Center for Mendelian Genomics [BHCMG], respectively).¹⁹ Y-axis, proportion of molecular diagnoses provided by variants in each gene; x-axis, genes; black, patients without CdLS listed as differential diagnosis; dark gray, patients with CdLS as one of the differential diagnoses; gray, CdLS cohort from ref. 19; light gray, CdLS cohort from BCHMG. **c** Comparison of genic variant frequencies between COSMIC and ExAC cohorts. Filled circles represent comparison between frequencies of putative loss-of-function (LoF) variants between COSMIC and ExAC; open circles represent comparison between frequencies of missense variants between COSMIC and ExAC. Y-axis, ratio between frequencies of genic variants (missense or putative LoF) in COSMIC and ExAC; x-axis, genes

cohesion cycle (Fig. 1a). Defects of the structural or regulatory components of cohesin lead to various multisystem malformation syndromes described as “cohesinopathies”, a collection of syndromes with shared clinical findings such as distinctive facial features, growth retardation, developmental delay/intellectual disability (DD/ID), and limb abnormalities. Clinically, the most distinguishable type of cohesinopathy is the classic Cornelia de Lange syndrome (CdLS, MIM #122470), with the majority of cases explained by single-nucleotide and insertion/deletion variants (SNVs/indels) and exonic copy-number variants (CNVs) resulting in loss-of-function (LoF) alleles in *NIPBL*.^{4–6} The traditional phenotype-driven studies that included the mild end of the CdLS spectrum led to the discovery of *SMC1A*, *SMC3*, *RAD21*, and *HDAC8* (MIM #300590, #610759, #614701, and #300882) as new cohesinopathy genes.^{4–11} The resultant CdLS phenotype is largely dependent on the genes being affected and pathogenic variant (PV) types.¹² Although mild forms of CdLS present with less striking phenotypes and are more clinically challenging to recognize in comparison with the classic form, they have been found in an increasing number of patients with cohesinopathies.

Here, we used a genotype-driven approach to investigate the allelic series of genes encoding cohesin components based on a large cohort of patients ($N = 10,698$) with a variety of unselected clinical presentations who were referred for clinical exome sequencing (CES). We identified pathogenic or likely pathogenic variants in known CdLS genes (*NIPBL*, *SMC1A*, *SMC3*, *RAD21*, and *HDAC8*) in patients mostly without a clinical diagnosis of CdLS, representing a cohort on the mild end of the clinical presentation of cohesinopathies. By applying the same genotype-first approach in the CES cohort, we further established *STAG1* and *STAG2* as new cohesinopathy genes with variants that act by a putative LoF mechanism, corroborating recent reports of patients with developmental disorders carrying PV in these two genes.^{13–15} Additional studies of patients who had chromosome microarray analyses (CMA, $N = 63,127$) also identified deletion CNVs affecting *STAG1* and *STAG2*, which further supports the human disease association of these two genes via a LoF

In addition to the aforementioned structural components, cohesin also interacts with the regulatory factors of the cohesion cycle, including proteins encoded by *NIPBL* (MIM #608667), *MAU2* (MIM #614560), *PDS5A* (MIM #613200) or *PDS5B* (MIM #605333), *WAPL* (MIM #610754), *HDAC8* (MIM #300269), *ESCO1* (MIM #609674), and *ESCO2* (MIM #609353), to facilitate cohesin dynamics and function on chromatin (Fig. 1a).^{1,2}

Precise orchestration of cohesin’s structural components and regulatory factors ensures faithful progression of the

Table 1 Summary of variants in the known Cornelia de Lange syndrome (CdLS) genes identified by Baylor Genetics clinical exome sequencing

Gene (transcript)	Genomic coordinates (hg19)	Exon /intron	Coding sequence change	Protein change	Zygoty	Inheritance	Novelty	Classification	CdLS as a differential diagnosis?	Dual molecular diagnosis?
NIPBL (NM_133433.3)	Chr5: 36985760	exon10	c.2479_2480del	p.R827Gfs*2	Het	De novo	Reported ³⁸	P	No (prenatal)	No
	Chr5: 37017173	exon24	c.4829T>C	p.L1610P	Het	De novo	This cohort	LP	No	No
	Chr5: 37046239	exon38	c.6527T>C	p.L2176P	Het	De novo	This cohort	LP	Yes	No
	Chr5: 37052580	exon42	c.7175G>A	p.C2392Y	Het	De novo	This cohort	LP	No	No
	Chr5: 36962223	intron5	c.459-2A>G	Splicing	Het	De novo	This cohort	P	Yes, among others, POC	No
	ChrX: 53442118	exon2	c.G110T	p.G37V	Het	De novo	This cohort	LP	No	No
	ChrX: 53442112	exon2	c.116C>G	p.S39*	Het	De novo	This cohort	P	Yes	MYH2 heterozygous c.1160C>T (p.A387V), de novo
SMC1A (NM_006306.2)	ChrX: 53442100	exon2	c.128A>T	p.D43V	Het	De novo	This cohort	LP	No	No
	ChrX: 53442088	exon2	c.140T>G	p.F47C	Het	De novo	This cohort	LP	No	CFTR homozygous c.1521_1523del (p.F508del)
	ChrX: 53441930	exon2	c.298G>C	p.G100R	Het	De novo	This cohort	LP	No	EFHC1 heterozygous c.1612C>T (p.R538*), paternally inherited
	ChrX: 53440211	exon4	c.586C>T	p.R196C	Hem	De novo	This cohort	LP	No	DMD hemizygous deletion exons 49–51, maternally inherited
	ChrX: 53440048	exon5	c.655del	p.A219Lfs*45	Het	De novo	This cohort	P	No	No
	ChrX: 53439899	exon5	c.802_804del	p.K268del	Het	De novo	Reported ³⁹	P	No	No
	ChrX: 53436051	exon9	c.1487G>A	p.R496H	Het	De novo	Reported ⁸	P	No	No
	ChrX: 53430523	exon15	c.2394dup	p.R799Tfs*4	Het	De novo	This cohort	P	No	No
	ChrX: 53430498	exon15	c.2420G>A	p.R807H	Het	De novo	This cohort	LP	No	No
	ChrX: 53426525	exon16	c.2547del	p.I849Mfs*12	Het	De novo	This cohort	P	No	No
	ChrX: 53423152	exon18	c.2853_2856del	p.S951Rfs*12	Het	De novo	Reported ⁴⁰	P	No	No
	ChrX: 53438853	intron7	c.1114-2A>G	Splicing	Hem	Maternal ^a	This cohort	P	No	No

Table 1 continued

Gene (transcript)	Genomic coordinates (hg19)	Exon /intron	Coding sequence change	Protein change	Zygoty	Inheritance	Novelty	Classification	CdLS as a differential diagnosis?	Dual molecular diagnosis?
SMC3 (NM_005445.3)	Chr10: 112341720	exon9	c.587T>C	p.I196T	Het	De novo	This cohort	LP	No	No
	Chr10: 112349688	exon15	c.1453_1455del	p.A485del	Het	De novo	This cohort	LP	No	No
	Chr10: 112356303	exon19	c.2111T>C	p.I704T	Het	De novo	This cohort	LP	No	No
	Chr10: 112362647	exon27	c.3362C>T	p.S1121F	Het	De novo	This cohort	LP	Yes	CREBBP heterozygous c.6137C>T (p.A2046V), de novo
	Chr8: 117862926	exon12	c.1550dupC	p.E518fs	Het	Paternal ^a	This cohort	P	No	No
RAD21 (NM_006265.2)	Chr8: 117866483	intron10	c.1161+1G>A	Splicing	Het	Maternal ^a	This cohort	P	No	No
	ChrX: 71787758	exon4	c.418G>A	p.G140R	Het	De novo	This cohort	LP	No	No
HDAC8 (NM_018486.2)	ChrX: 71715066	exon5	c.490C>T	p.R164* ^b	Het	De novo	Reported ⁷	P	No	No
	ChrX: 71715066	exon5	c.490C>T	p.R164* ^b	Het	De novo	Reported ⁷	P	No	No
	ChrX: 71715029	exon5	c.527A>G	p.D176G	Het	De novo	This cohort	LP	No	RFX5 compound heterozygous c.1362_1368delinsGT (p.K455fs) and c.240_242delCTC (p.S81del)
	ChrX: 71710823	exon6	c.584T>A	p.V195D	Het	De novo	This cohort	LP	No	No
	ChrX: 71684526	exon8	c.793G>A	p.G265R	Het	De novo	This cohort	LP	No	No
71681927	ChrX: 71681927	exon9	c.932C>T	p.T311M	Het	De novo	Reported ⁷	P	No	No
	ChrX: 71681922	exon9	c.937C>T	p.R313*	Het	Not maternal	This cohort	P	No	No

^aP pathogenic, LP likely pathogenic, POC product of conception

^bInherited variants from mildly affected parents, who were confirmed to be nonmosaic by Sanger sequencing (data not shown)

^cIdentical pathogenic variants in unrelated patients

mechanism. We also provide evidence supporting the candidacy of *PDS5A* and *WAPL* as cohesinopathy disease genes. Our findings emphasize the utility of CES to provide molecular diagnoses for disorders with extensive genetic and phenotypic heterogeneity, uncover the potential molecular etiologies of previously undiagnosed patients, and elucidate novel candidate cohesinopathy disease genes that potentially expand the genotype/phenotype characterizations of cohesinopathies.

MATERIALS AND METHODS

Samples

The study has been conducted through a collaborative effort between Baylor Genetics (BG) and Baylor-Hopkins Center for Mendelian Genomics (BHCMG), and has been approved by the Institutional Review Board of Baylor College of Medicine. Approved consents for publishing photos have been obtained. Please see Supplemental Appendix for detailed descriptions of samples in BG and BHCMG. Selected patients with *STAG1*, *STAG2*, or *PDS5A* variants were enrolled after obtaining informed consent for further phenotypic characterization based on clinical notes submitted along with the CES order.

CES and variant interpretation

CES was performed as previously described.^{16,17} The variant classification and interpretation were conducted by a clinical standard based on the American College of Medical Genetics and Genomics variant interpretation guidelines.¹⁸ Details of the CES experimental procedures and sample-wise quality control (QC) metrics can be found in Table S1. The possibility of mosaic variants in known CdLS genes¹⁹ was carefully evaluated. A variant is considered mosaic only if the variant read versus total read ratio is below 30% and confirmatory Sanger sequencing demonstrates a comparable mosaic fraction.

The variants identified in this study have been deposited to ClinVar (accession numbers SCV000747051-SCV000747088 and SCV000747090-SCV000747093).

Chromosome microarray analysis

The experimental design and data analysis of chromosome microarray analysis (CMA) were performed according to previously described procedures.²⁰

X-chromosome inactivation assay

X-chromosome inactivation (XCI) studies were performed for the patient samples with *STAG2* variants based on the protocol described by Allen *et al.*²¹ with modifications. Please see Supplemental Appendix for detailed protocols.

Estimation of pathogenic variant prevalence in somatic cancer samples

The datasets from the COSMIC (<http://cancer.sanger.ac.uk/cosmic/download>) and ExAC (Exome Aggregation Consortium, <http://exac.broadinstitute.org/>)²² databases were used for the calculation. The normalized PV abundance per gene in

cancer samples is determined by the ratio between the PV frequencies of COSMIC versus the ExAC (y -axis in Fig. 1c). Please see Supplemental Appendix for details.

RESULTS

Variants of established CdLS genes in the CES cohort

Based on a genotype-driven selection approach, we identified 33 patients with pathogenic or likely pathogenic variants in the well-recognized CdLS genes from the CES cohort. Those variants include heterozygous or hemizygous SNVs/indels in *NIPBL* ($N=5$), *SMC1A* ($N=14$, X-linked), *SMC3* ($N=4$), *RAD21* ($N=2$), and *HDAC8* ($N=8$, X-linked) (Table 1). Genic variant distribution was calculated to show the per-gene contribution to molecular diagnosis among the five known CdLS genes (Fig. 1b). Of the 33 variants, 29 occurred *de novo* in the proband, 3 were inherited from a parent, and 1 was of unknown inheritance (not maternally inherited, paternal sample not available, Table 1). Among the inherited variants, one variant in *SMC1A* was inherited from a symptomatic mother with a milder phenotype, demonstrating variable clinical presentation for X-linked dominant disorders; two variants in *RAD21* were inherited from symptomatic parents with milder phenotypes, documenting variable expressivity of defects in *RAD21*.

The CdLS patients in this cohort may be enriched for atypical or mild CdLS phenotypes, because those with classic CdLS presentation are more likely to be referred for specific single-gene or panel testing instead of CES. We retrospectively examined the clinical notes submitted by the referral clinicians for their differential diagnoses prior to CES. CdLS was not included in the initial differential diagnoses for 60% of patients with a positive *NIPBL* finding, 93% with *SMC1A*, and 75% with *SMC3* variants, and all those with *RAD21* or *HDAC8* variants (Table 1, Fig. 1b). These observations support the previous hypotheses that pathogenic variants in *NIPBL* have a better correlation with classic CdLS, while *SMC1A* and *SMC3* pathogenic variants may contribute to milder CdLS features; the phenotypes caused by pathogenic variants in *RAD21* and *HDAC8* become more variable and sometimes present atypical CdLS features.¹²

As a comparison with the genic distribution of our CES cohort, we analyzed the data from a phenotype-driven cohort of CdLS patients.¹⁹ Moreover, we re-examined the genic variant distribution on an independent phenotype-driven CdLS cohort ($N=41$) from BHCMG, in which pathogenic or likely pathogenic variants in *NIPBL* ($N=12$), *SMC1A* ($N=6$), *SMC3* ($N=2$), and *HDAC8* ($N=1$) were identified (Table S2). The genic variant distribution of the BHCMG CdLS cohort is overall comparable with that calculated from the phenotype-driven cohort.¹⁹ However, both of these largely deviated from our CES cohort (Fig. 1b). The proportion of patients with *NIPBL* pathogenic variants in our cohort was significantly lower in comparison with the aforementioned two phenotype-driven cohorts (chi-squared test, both with $p < 0.001$). The proportion of patients with *SMC1A* pathogenic variants in our cohort and the BHCMG were significantly

higher than the other CdLS cohorts (chi-squared test, both with $p < 0.02$), indicating mild/atypical CdLS presentations in the BHCMG cohort. Therefore, the mutational spectrum in known CdLS genes in the CES cohort represent a distinct distortion and alternative perspective from phenotype-driven CdLS cohorts, where patients tend to present with classic phenotypes.¹¹

Interestingly, 6/33 (18%) of the patients with positive findings from known CdLS genes carry a secondary diagnosis (Table 1), which is higher than the average observed fraction of patients with dual diagnoses from positive cases in the entire CES cohort (~5%) (ref. 23). This is not unexpected because the predicted extent of multilocus diagnosis can be as high as 14% under a Poisson distribution model.²³ The high representation of dual diagnosis and resultant blended phenotypes observed in this study may contribute to the complexity of the patients' phenotypes, further obscuring the underlying molecular causes, making clinical diagnosis challenging without the assistance from objective molecular testing.

Candidate disease genes in the cohesin structural and regulatory components

STAG1, *STAG2*, *PDS5A*, *PDS5B*, *WAPL*, and *MAU2* encode close interacting factors of NIPBL, SMC3, SMC1A, RAD21, and HDAC8 in the cohesin pathway, and thus may potentially supplement the locus heterogeneity of cohesinopathies. According to the ExAC database, *NIPBL*, *SMC3*, *SMC1A*, and *RAD21* have probability of LoF intolerance (pLI) scores of 1.00, while *HDAC8* has a pLI of 0.92. Similarly, *STAG1*, *STAG2*, *PDS5A*, *PDS5B*, *WAPL*, and *MAU2* all have pLI scores of 1.00, suggesting their intolerance to LoF variants (Table S3). In our CES cohort, we identified putative LoF (truncating/splicing) or de novo missense variants in *STAG1* (3), *STAG2* (2), *PDS5A* (2), and *WAPL* (1). Through collaboration with the Deciphering Developmental Disorder (DDD) study and BHCMG, three additional de novo variants in *STAG2* were identified.

De novo heterozygous SNVs/indels in *STAG1* (NM_005862.2), including one frameshift variant (c.2009_2012del [p.N670Ifs*25]) and one missense variant (c.1129C>T [p.R377C]), were identified in patients 1 and 2, respectively (Fig. 2a). Both patients had common clinical findings that included DD/ID, hypotonia, seizures, mild dysmorphic features, and skeletal abnormalities (Table 2, Table S4). In addition, one heterozygous de novo missense SNV, c.253G>A (p.V85I) in *STAG1*, was identified in patient 3 (Fig. 2a) along with a heterozygous de novo c.1720-2A>G SNV (observed twice in ExAC including one potentially being mosaic) in *ASXL1* (Bohring–Opitz syndrome; MIM #605039). Patient 3 presented with global developmental delay, dysmorphic facial features, seizures, optic atrophy, mild hypotonia, skin hypopigmentation, hirsutism, possible autism spectrum disorder, and structural brain abnormalities (Table 2, Table S4). The concurrent de novo variants in

STAG1 and *ASXL1* could possibly contribute to a dual molecular diagnosis of this patient.

De novo heterozygous/hemizygous SNVs/indels in *STAG2* (X-linked, NM_006603.4), including two stopgain variants, two missense variants, and one frameshift variant, were identified in four females (patients 7–10; patient 7, c.418C>T [p.Q140*]; patient 8, c.1605T>A [p.C535*]; patient 9, c.1811G>A [p.R604Q]; patient 10, c.1658_1660delinsT [p.K553Ifs*6]); and one male (patient 11 [hemizygous], c.476A>G [p.Y159C]) (Fig. 2b). These patients shared common clinical findings of DD/ID, hypotonia, microcephaly, dysmorphic features, and skeletal abnormalities (Table 2, Table S4). Skewed X-inactivation (XCI) was observed in patient 8, whereas XCI was noninformative for patient 7 due to homozygosity of the marker being used for the XCI study (data not shown). In our study, truncating variants were identified in 3/4 female patients, but not in males. Although this observation is based on a limited number of patients, it is consistent with the hypothesis that truncating variants of X-linked genes may impose more severe pathogenic effect on males than females.

One heterozygous SNV, c.2275G>T (p.E759*), in *PDS5A* (NM_001100399.1) was identified in patient 13 with severe developmental delay, marked hypotonia, failure to thrive, dysmorphic features, hyperextensible knees, eye anomalies, and skeletal abnormalities (Table 2, Table S4). Interestingly, this patient also had a concurrent heterozygous de novo SNV, c.3325A>T (p.K1109*), in *ASXL3* (Bainbridge–Ropers syndrome, MIM #615485), which presumably explains the major phenotypes. This *PDS5A* variant is predicted to introduce a premature stop codon in *PDS5A* in the longer transcript (NM_001100399.1) but does not affect the shorter transcript (NM_001100400.1), suggesting a potential mild defect caused by this variant. However, the role of different isoforms of *PDS5A* in the cohesin complex is not well established in the literature. Notably, the father of patient 12, who shared the *PDS5A* p.E759* variant, had speech impediment. Although the pathogenicity of the p.E759* variant in *PDS5A* remains to be investigated, it may modulate the patient's phenotype and constitute a dual diagnosis together with *ASXL3*. In addition, one heterozygous de novo SNV (c.654+5G>C) in *PDS5A* was identified in another patient with neurodevelopmental disorders. This intronic *PDS5A* variant was predicted to affect splicing of the major messenger RNA (mRNA) transcript of *PDS5A* by prediction programs including SpliceSiteFinder-like and MaxEntScan (<http://www.interactive-biosoftware.com/doc/alamut-visual/2.6/splicing.html>).

Finally, one de novo heterozygous SNV in *WAPL* (NM_015045.3), c.2192G>A (p.R731H), was identified in one patient with neurodevelopmental disorders. This observation corroborates a previous report in which a partial duplication involving *WAPL* was identified in a patient from a phenotype-driven CdLS cohort,²⁴ providing further evidence for *WAPL* as a candidate disease gene.

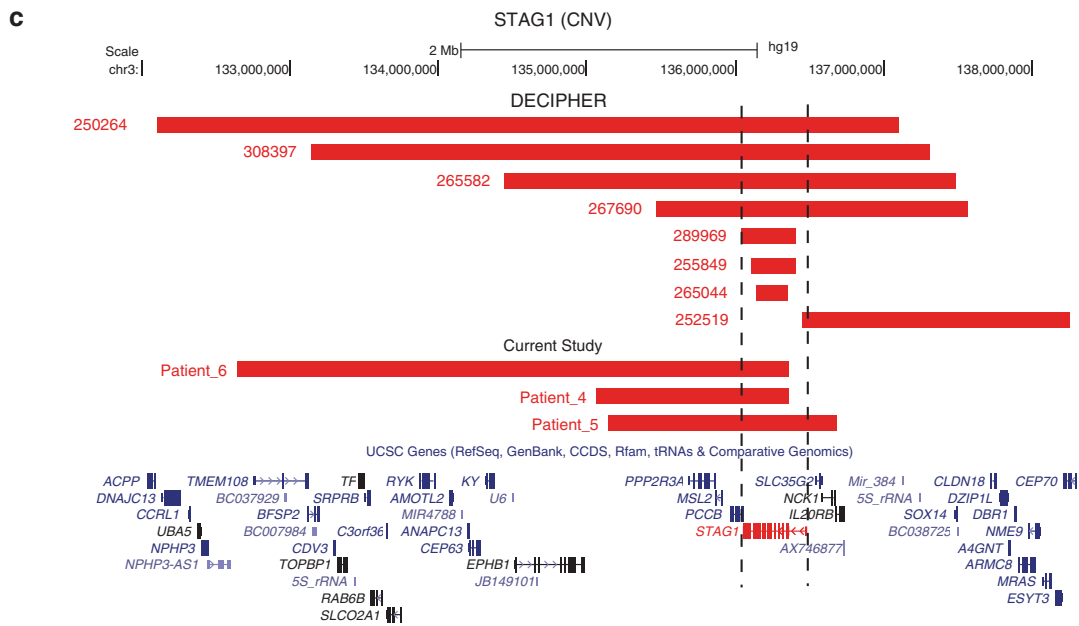
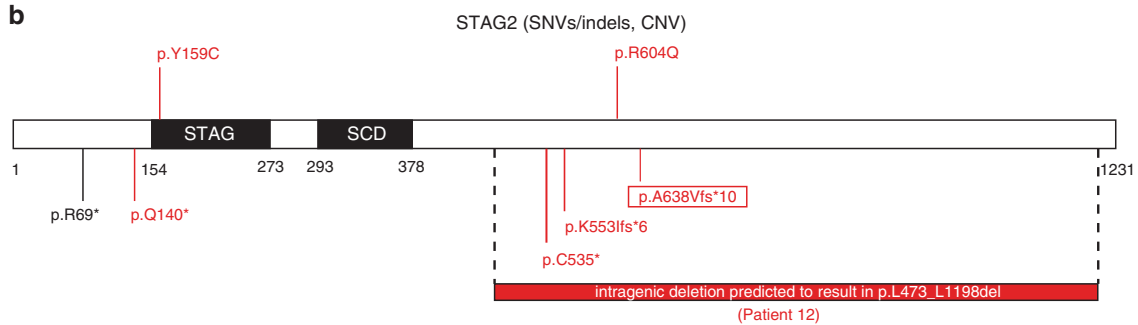
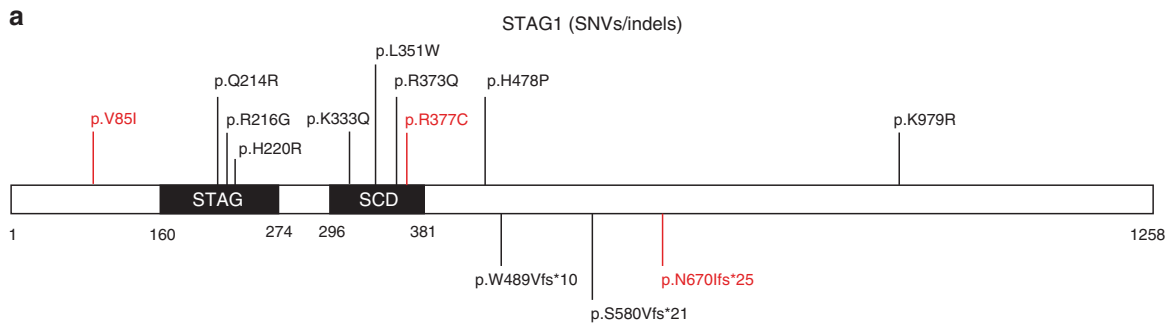


Fig. 2 The variants in *STAG1* and *STAG2*. **a** Single-nucleotide variants (SNVs)/indels in *STAG1*. **b** SNVs/indels and one copy-number variant (CNV) deletion in *STAG2*. For panels **a** and **b**, the white segment represents the full-length protein, and the black segments represent protein domains; the missense variants are annotated above the segment, while the putative loss-of-function (LoF) variants (including the CNVs deletion in *STAG2*) are underneath; the variants colored in red are reported in the current study. The boxed variant (p.A638Vfs*10) in panel **b** is reported as a research variant. **c** Diagram showing the CNV deletions overlapping *STAG1* reported in DECIPHER and the current study. The red segments represent the deletions, which are divided in two groups: DECIPHER and Current Study. The bottom panel shows genes in the region. *STAG1* is highlighted in red. **d** Photographs showing the front and side facial profiles of patients 8 and 9 with de novo variants in *STAG2*. The patient numbers and variants are listed under the photograph

Each of the variants in *STAG1*, *STAG2*, *PDS5A*, and *WAPL* described above were not observed in the control population databases including ExAC and ESP5400 (National Heart, Lung, and Blood Institute [NHLBI] Exome Sequencing Project, <http://evs.gs.washington.edu/EVS/>). The interpretation of deleterious effects of the de novo missense SNVs identified in this study was supported by multiple prediction algorithms (Table S5).

We identified CNV deletions affecting *STAG1* and *STAG2* in our clinical CMA cohort, supporting LoF as the presumed disease-contributing mechanism; no putative LoF CNVs of *PDS5A*, *PDS5B*, *WAPL*, or *MAU2* were identified. In total, we identified three CNV deletions affecting *STAG1* (two de novo, one of unknown inheritance) in patients with developmental disorders (Fig. 2c, Table S6). In the literature, six CNV deletions overlapping *STAG1* were reported, with the smallest two deletions being intragenic (exons 2–5 and exons 13–18, respectively).¹³ Moreover, eight cases with neurodevelopmental disorders were reported in the DECIPHER database harboring relatively small-sized deletions (<5 Mb) affecting *STAG1* (<https://decipher.sanger.ac.uk/>)²⁵ (Fig. 2c, Table S6). These *STAG1*-overlapping deletions identified in affected patients strongly indicate that haploinsufficiency is likely to be the disease-contributing mechanism for *STAG1*. In addition, a 33.9-Kb CNV deletion with unknown inheritance encompassing exons 15–32 of *STAG2* (predicted to result in an in-frame deletion p.L473_L1198del), was identified in patient 12 with dysmorphic features, microcephaly, and seizures (Fig. 2b, Table S6). This female patient showed skewed XCI, consistent with the observation in patient 8.

Patients with *STAG1* and *STAG2* variants have phenotypes overlapping the CdLS spectrum

We evaluated the clinical phenotypes for patients 1–2 (*STAG1*) and patients 7–11 (*STAG2*). Patient 3 (*STAG1*) was excluded from the evaluation because the identification of concurrent de novo variants in *ASXL1* together with *STAG1* may largely complicate the *STAG1*-alone phenotypes.

Patients described in this paper presented for genetic evaluation due to developmental delay and/or congenital anomalies but not with classic distinctive facial features or a recognizable pattern of malformation suggestive for a particular syndrome such as CdLS (Fig. 2d). The most common features among these patients with *STAG1* and *STAG2* variants were DD/ID, behavioral problems, hypotonia, seizures, microcephaly, failure to thrive, short stature, mild dysmorphic features, and 2–3 toe syndactyly (Table 2).

Clinical profiling suggested many overlapping features with CdLS, which include DD/ID, growth failure including short stature and microcephaly, hearing loss, synophrys, micrognathia, limb anomalies, and hypoplastic male genitalia. Some other less common features of CdLS, such as cutis marmorata, myopia, congenital diaphragmatic hernia (CDH), and renal anomalies, among others, were also observed in several of these patients. A more detailed characterization is described in Table 2 and Table S4.

Among the distinctive craniofacial features present in over 95% of the patients with a clinical diagnosis of CdLS,¹¹ our patients collectively had microbrachycephaly, low-set ears, synophrys, long curly eyelashes, broad nasal bridge, anteverted nares, long and smooth philtrum, thin upper lip, and micrognathia; however, these features were not present concurrently in a single patient. Interestingly while microcephaly is one of the most characteristic features in CdLS, only 4/7 patients (one *STAG1* and three *STAG2*) had microcephaly. Although the numbers are small, a higher percentage of microcephaly was observed in patients with a *STAG2* variant (3/5) in comparison with *STAG1* (1/2). In contrast to CdLS, where mild to severe limb anomalies are common and are usually helpful to establish a clinical diagnosis, the patients in this study had common but more subtle findings in their extremities, such as fifth finger clinodactyly and syndactyly. Skeletal anomalies including scoliosis (3/7), vertebral anomalies (3/7), and rib fusion (2/7) were observed in our patients, all with variants in *STAG2*. Even though these skeletal anomalies can be observed in patients with classic CdLS, vertebral and rib anomalies would be considered as rare or atypical features for CdLS.

Comparing patients with *STAG1* or *STAG2* variants, DD/ID and mild dysmorphic features have been consistently observed, which is in line with the previous reports^{13–15} (Table 2). Despite the small cohort size, it seems that patients with *STAG2* variants have more multisystem congenital anomalies such as CDH, congenital heart disease, and vertebral anomalies. Growth failure was observed as well, but apparently more in the postnatal period than prenatally. Patients with a *STAG2* variant appear to have more severe growth failure especially in weight and length parameters compared with those with *STAG1* variants.

Although *STAG1* and *STAG2* have been implicated in cancers due to their function in the cohesin pathway and the observation of chromosomal segregation defects in defective cell lines (e.g., *STAG2* as an indicator for myeloid neoplasms), onset of tumors has not been observed in our study nor in the patients reported in the literature with developmental

Table 2 Genotypes and phenotypes of patients with SNVs/indels in STAG1, STAG2, and PDS5A identified in current study

Genes	STAG1 (NM_005862.2)					STAG2 (NM_006603.4)					PDS5A (NM_001100399.1)	
	Patient 1	Patient 2	Patient 3	Reported in Ref. 13 (n=17)		Patient 7	Patient 8	Patient 9	Patient 10	Patient 11		Reported in Ref. 14 (n=1)
Patients												
Age at last exam	11 years 5 months	4 years 8 months	4 years 2 months	30 months to 33 years (median 7 years)		3 years 8 months	4 years 6 months	11 years 1 month	1 year 11 months	5 years 3 months	8 years	Patient 13 2 years 6 months
Variant	c.2009_2012del (p.N670fs*25)	c.1129C>T (p.R377C)	c.253G>A (p.V85I), STAG1 c.1720-2A>G: ASXL1;	CNV deletion or SNVs/indels		c.418C>T (p.Q140*)	c.1605T>A (p.C535*)	c.1811G>A (p.R604Q)	c.1658_1660delinsT (p.K553ifs*6)	c.476A>G (p.Y159C), hemizygous	c.205C>T p. (Arg69*)	c.2275G>T (p.E759*); PDS5A c.3325A>T (p.K1109*); ASXL3 ASXL3, PDS5A
Critical gene(s)	STAG1	STAG1	ASXL1, STAG1	STAG1 and others ^a		STAG2	STAG2	STAG2	STAG2	STAG2	STAG2	ASXL3, PDS5A
Gender	F	M	F	9M/8F		F	F	F	F	M	F	F
Inheritance	De novo	De novo	Both de novo	De novo or inherited		De novo	De novo	De novo	De novo	De novo	De novo	ASXL3: de novo; PDS5A: paternal
Growth	-	NR	-	3/17		-	+	-	-	+	-	+
	-	+	-	1/17		NR	+	+	+	+	NR	+
	-	+	-	5/17		NR	+	+	+	+	+	+
	-	+	-	4/17		-	+	+	+	+	+	+
Development	+	NR	+	17/17, mild to severe		NR	+	+	+	+	+	+
	+	+	+	17/17		+	+	+	+	+	+	+
	NR	NR	+	7/17		NR	NR	NR	NR	NR	-	-
Neurobehavioral	NR	+	+	NR		NR	+	NR	+	+	+	NR
Behavioral problems	NR	+	+	NR		NR	+	NR	+	+	+	NR
Seizures	NR	+, during infancy	+	7/17 with epilepsy		Myoclonic movements	NR	NR	+	-	NR	-
Hypertonia	NR	-	-	NR		NR	NR	NR	-	-	NR	+
Hypotonia	NR	+	+	NR		NR	+	+	+	+	NR	-
Brachycephaly	NR	NR	-	See footnotes ^b		-	+	+	+	NR	See footnotes ^c	-
Long curly eyelashes	+	NR	-	See footnotes ^b		NR	+	+	+	-	See footnotes ^c	-
Synophrys	NR	NR	+	See footnotes ^b		NR	NR	-	-	-	See footnotes ^c	-
Anteverted nares	NR	NR	+	See footnotes ^b		-	NR	+	+	+	See footnotes ^c	-
Depressed/broad nasal bridge	NR	+	+	See footnotes ^b		-	-	+	+	+	See footnotes ^c	+
Bulbous nasal tip	NR	NR	-	See footnotes ^b		-	NR	+	+	+	See footnotes ^c	-
Low-set ears	+	-	-	See footnotes ^b		+	NR	+	+	+	See footnotes ^c	-
Dysmorphic ears	+	-	-	See footnotes ^b		+	NR	+	+	+	See footnotes ^c	-
Long/smooth philtrum	-	NR	-	See footnotes ^b		NR	+	+	-	-	See footnotes ^c	-
High arched palate	NR	+	+	See footnotes ^b		-	-	NR	+	NR	See footnotes ^c	+
Thin upper lip	NR	NR	-	See footnotes ^b		+	+	+	+	+	See footnotes ^c	-
Downturned mouth	NR	NR	-	See footnotes ^b		NR	NR	+	+	-	See footnotes ^c	-
Cleft lip/palate	+	-	-	See footnotes ^b		-	-	NR	+	+	See footnotes ^c	-
Widely spaced teeth	NR	NR	+	See footnotes ^b		NR	NR	+	+	-	See footnotes ^c	-
Micrognathia	NR	+	-	See footnotes ^b		NR	+	+	+	-	See footnotes ^c	-
Hypoplastic nails	-	NR	-	NR		NR	NR	NR	+	-	See footnotes ^c	-
Hirsutism	NR	NR	+	NR		NR	NR	NR	+	-	See footnotes ^c	-
Hairline	NR	NR	-	NR		NR	Low, posterior	NR	NR	NR	low, anterior	-
Cutis marmorata	+	NR	-	NR		NR	+	NR	NR	-	NR	-
Strabismus	+	NR	+	NR		NR	+	NR	NR	-	NR	-
Hearing loss	-	-	-	NR		NR	+	NR	NR	-	NR	-
Cardiovascular	-	PDA	-	1/17		+	NR	-	NR, no murmur	Minimal PFO, normal on follow-up	+	-
Congenital heart defect	-	-	-	NR		+	NR	+, right	-	NR	NR	-
Respiratory/thorax	-	NR	-	NR		NR	NR	+	+	NR	NR	-
Congenital diaphragmatic hernia	-	NR	-	NR		NR	NR	+	+	NR	NR	-
Pulmonary hypoplasia	-	NR	-	NR		NR	NR	+	+	NR	NR	-

Table 2 continued

Genes	STAG1 (NM_005862.2)	STAG2 (NM_006603.4)	PDSSA (NM_001100399.1)
Gastrointestinal reflux	NR	NR	NR
Genitourinary/ Renal Anomaly	NR	+, Nissen and G-tube	NR
Gastroesophageal reflux	NR	+	-
Hypoplastic male genitalia	NA	NA	NA
Cryptorchidism	NA	NA	NA
Structural anomalies of the renal tract	+, left kidney examined	NR	+, single kidney
Musculoskeletal/ extremities	-	+	NR
Scoliosis	-	NR	NR
Rib fusion	NR	+, T4-5, T10-11, BL	NR
Vertebral anomalies	NR	NR	NR
Arm/hand anomalies	NR	+, vertebral clefts	NR
Limited elbow extension	+	NR	NR
Fifth finger clinodactyly	+	NR	NR
Single transverse palmar crease	NR	NR	NR
2-3 toe syndactyly	+	NR	NR
Abnormal brain MRI	+	NR	Ectopic posterior pituitary, short pituitary stalk
Studies and imaging	3/17 showed atrophy; other 17 showed unspecific anomaly	NR	+
Abnormal	NR	NR	+

BL, bilateral, CA coarctation of the aorta, IUGR intrauterine growth retardation, NA not applicable, NR no record, PDA patent ductus arteriosus, PS pulmonary stenosis, VSD ventricular septal defect, PFO patent foramen ovale, CNV copy-number variant, SNV, single-nucleotide variant, MRI magnetic resonance image

*STAG1 was affected by both CNV deletion and SNVs/indels. The deletions included three de novo and one with unknown parent of origin, which encompassed STAG1 and PCCB; one intragenic, which was absent in the mother; and two intragenic, which were maternally inherited; the SNVs/indels included eight de novo missense and two de novo frameshift variants of STAG1. ^b Facial features included 14/17 with deep-set eyes, 13/17 with wide mouth, 7/17 with high nasal bridge, 8/17 with thin eyebrows, 4/17 with widely spaced central incisors; Micrognathia, ear abnormalities, wide-set eyes, beaked or prominent nose, arched eyebrows, or low-set ears, cleft/arched palate

disorders caused by constitutional pathogenic variants in *STAG1* and *STAG2* (refs.13–15). Moreover, no obvious increased risk of cancer is reported in patients with other cohesinopathies caused by defects in genes such as *NIPBL*, *SMC1A*, and *SMC3* (ref. 1). Consistent with this observation, our chromosome analysis of one patient (patient 7) did not reveal any evidence for chromosomal segregation defects (data not shown).

DISCUSSION

In this study, we applied a genotype-driven approach to decipher the genetic causes of cohesinopathy from a CES perspective. We describe a series of disease-contributing variants in known cohesinopathy genes, and also provide molecular evidence supporting the candidacy of recently described or new disease genes.

NIPBL defects are underrepresented in this cohort likely due to ascertainment bias associated with its more clinically recognizable presentations. The scarcity of putative LoF variants for certain cohesin genes including *PDS5B* and *MAU2* in this cohort indicates that LoF variants in these genes may exert strong pathogenic effects on early development leading to incompatibility with life. Alternatively, the lack of evidence supporting the pathogenicity of variants in *PDS5B* and *MAU2* could reflect limitations of interpreting missense variants based on proband-only CES. *HDAC8* and *SMC1A* are the only two well-studied X-linked genes among the cohesin components. They seem to be relatively spared from the strong selection in human development possibly due to protection of pathogenic alleles in the gene pool by XCI in females. Consistently, variants in these two genes are highly represented in the CES cohort as compared with cohorts assembled by phenotypic characterization (Fig. 1b).

Patients harboring *STAG1* or *STAG2* variants seem to share many of the clinical features seen in the well-described CdLS phenotype. Apparently affected patients in our cohort are developmentally and intellectually as impaired as those with CdLS. However, their spectrum of growth, craniofacial, and musculoskeletal features are not as severe as the spectrum of CdLS. Overall, only one patient (patient 3 [*STAG1*]) fulfills the diagnostic criteria for CdLS by meeting the CdLS characteristic facial features.²⁶ Note that the concurrent *de novo* variant in *ASXL1* may largely contribute to the differential diagnosis of CdLS for patient 3 (Table S7). Although the currently available clinical information we had might not be as sufficient for a diagnosis of CdLS or other cohesinopathies, a “CdLS-like” syndrome started to emerge. The *STAG1/STAG2*-related disorders seem to be at the mild end of the CdLS spectrum, making the clinical diagnosis for these two genes more challenging for physicians. Putting together the constellation of clinical features might help to end the diagnostic odyssey earlier, and with this series of cases awareness can be extended. Given the challenges, comprehensive genomic analysis, such as CES, should be offered to efficiently provide a molecular diagnosis for these cohesinopathy conditions.

Notably, the LoF *PDS5A* variant (patient 13) was inherited from a father with speech impediment. Although the phenotypic consequence of this variant remains unclear (as discussed in Results), its potential contribution cannot be completely ruled out. Unfortunately, samples from the paternal grandparents or other relatives are not available for testing. Defects in the cohesin complex, as demonstrated in the CdLS genes, are likely to be detrimental to proper organismal development, and milder phenotypic consequences have been observed.¹¹ With our experience of known CdLS gene variants among 10,698 individuals, two distinct novel pathogenic variants in *RAD21* as well as one novel pathogenic variant in *SMC1A* (X-linked) were identified in three unrelated patients with neurodevelopmental disorders, all inherited from affected parents with milder phenotypes (Table 1). Moreover, transmission of a pathogenic variant between generations has been reported in *STAG1* (ref. 13). Therefore, with the reported variable expressivity of the cohesin defects, it is plausible that the reproductive potential, genetic transmission, and severity of phenotype may be dependent on various factors, including the components being affected, the PV types, the inheritance mode (e.g., X-linked or autosomal dominant), and the downstream pathways disrupted by defects in a particular component. Thus, additional genotype–phenotype correlation studies are warranted to further delineate the spectrum of cohesinopathies.

The mutational landscape of cohesin genes in somatic cancer may represent an alternative view to reflect contribution of these genes to biological processes, with minimum selection as compared with that imposed during early human development. Among cancer samples deposited to the COSMIC database subjected to genome-wide screening, truncating variants were observed in all cohesin genes. While missense variants did not show any substantive difference between cohesin genes, putative LoF variants in *STAG2* were highly represented in the somatic cancer cohort (Fig. 1c). LoF variants in *STAG2* have been significantly associated with several cancers,^{27,28} suggesting a likely pleiotropic effect of *STAG2*, possibly with strong involvement in tumorigenesis. Interestingly, we have observed a patient with mosaic *STAG2* LoF variant in the CES cohort. The patient does not have neurodevelopmental problems, but instead presented with hematological malignancy. Therefore, we considered the *STAG2* defect in this patient as not being causal for a cohesinopathy. Consequently, caution should be taken when interpreting variants in cohesin genes by considering the possibility that they may arise as somatic changes after the critical period of early human development.

Accumulating evidence suggests that cohesin contributes to the topological organization of the genome, regulates DNA replication, and facilitates long-range gene transcription regulation.^{2,29,30} In addition, the interactions between cohesin and other transcription machinery and chromatin remodeling complexes to recognize specific genomic loci and regulate gene transcription have aggregated these complexes into the same pathways of transcription regulation.^{30–33} Notably,

genes encoding components of chromosome remodeling and transcription regulation machineries, such as *ANKRD11*, *AFF4*, *KMT2A*, *TAF1*, and *TAF6*, have been associated with phenotypes reminiscent of CdLS.^{3,19,34–36} Such findings expand the molecular mechanism underlying cohesinopathies into transcriptional regulation. Interestingly, gene expression studies of patients with elevated dosage of *STAG2* reveal a dysregulated transcriptome and pinpoint altered expression levels of developmentally important genes.³⁷ Therefore, the versatility of cohesin in cohesion and transcription regulation warrants a further investigation of its downstream effectors.

In summary, the genotype-first approach focusing on a specific pathway enabled us to investigate patients with nonclassic cohesinopathy phenotypes; this approach also allowed us to discover patients with variants in new or recently reported disease genes, namely *STAG1*, *STAG2*, and potentially *PDS5A* and *WAPL*, which may further expand the genetic heterogeneity underlying cohesinopathies. Future studies of cellular phenotypes, with regard to functional studies of DNA repair and transcriptome analysis, are warranted to further elucidate the mechanistic consequences due to defects in specific cohesin components, which may shed light on precision medicine efforts targeting distinct molecular pathways.

ELECTRONIC SUPPLEMENTARY MATERIAL

The online version of this article (<https://doi.org/10.1038/s41436-018-0085-6>) contains supplementary material, which is available to authorized users.

ACKNOWLEDGEMENTS

This study was supported in part by the National Human Genome Research Institute/National Heart, Lung, and Blood Institute (NHGRI/NHLBI) grant UM1HG006542 to the BHCMG; and National Institutes of Neurological Disorders and Stroke (NINDS) grant R35 NS105078-01 to JRL. JEP was supported by the NHGRI grant K08 HG008986. AHC, ELB and LR are supported by Newlife (Ref:16-17/12). We acknowledge Dr. Sureni V. Mullegama for critical comments on this manuscript. This study makes use of data generated by the DECIPHER community. A full list of centers that contributed to the generation of the data is available from <http://decipher.sanger.ac.uk> and via e-mail from decipher@sanger.ac.uk. Funding for the project was provided by the Wellcome Trust. The DDD study presents independent research commissioned by the Health Innovation Challenge Fund (grant number HICF-1009-003), a parallel funding partnership between the Wellcome Trust and the Department of Health, and the Wellcome Trust Sanger Institute (grant number WT098051). The views expressed in this publication are those of the author(s) and not necessarily those of the Wellcome Trust or the Department of Health. The study has UK Research Ethics Committee (REC) approval (10/H0305/83, granted by the Cambridge South REC, and GEN/284/12 granted by the Republic of Ireland REC). The research team acknowledges the support of the National Institute for Health Research, through the Comprehensive Clinical Research Network.

DISCLOSURE

Baylor College of Medicine (BCM) and Miraca Holdings Inc. have formed a joint venture with shared ownership and governance of Baylor Genetics (BG), formerly the Baylor Miraca Genetics Laboratories (BMGL), which performs chromosomal microarray analysis and clinical exome sequencing. JR, VP, WJ, CS, WB, SWC, AMB, JLS, CE, YY, RX, and PL are employees of BCM and derive support through a professional services agreement with the BG. JRL serves on the Scientific Advisory Board of the BG. JRL has stock ownership in 23andMe, is a paid consultant for Regeneron Pharmaceuticals, has stock options in Lasergen, Inc., and is a co-inventor on multiple United States and European patents related to molecular diagnostics for inherited neuropathies, eye diseases, and bacterial genomic fingerprinting. The other authors declare no conflict of interest. All authors read and approved the final manuscript.

REFERENCES

- Liu J, Krantz ID. Cornelia de Lange syndrome, cohesin, and beyond. *Clin Genet*. 2009;76:303–14.
- Losada A. Cohesin in cancer: chromosome segregation and beyond. *Nat Rev Cancer*. 2014;14:389–93.
- Yuan B, Pehlivan D, Karaca E, et al. Global transcriptional disturbances underlie Cornelia de Lange syndrome and related phenotypes. *J Clin Invest*. 2015;125:636–51.
- Krantz ID, McCallum J, DeScipio C, et al. Cornelia de Lange syndrome is caused by mutations in NIPBL, the human homolog of *Drosophila melanogaster* Nipped-B. *Nat Genet*. 2004;36:631–5.
- Pehlivan D, Hullings M, Carvalho CM, et al. NIPBL rearrangements in Cornelia de Lange syndrome: evidence for replicative mechanism and genotype-phenotype correlation. *Genet Med*. 2012;14:313–22.
- Tonkin ET, Wang TJ, Lisgo S, et al. NIPBL, encoding a homolog of fungal Scc2-type sister chromatid cohesion proteins and fly Nipped-B, is mutated in Cornelia de Lange syndrome. *Nat Genet*. 2004;36:636–41.
- Deardorff MA, Bando M, Nakato R, et al. HDAC8 mutations in Cornelia de Lange syndrome affect the cohesin acetylation cycle. *Nature*. 2012;489:313–7.
- Deardorff MA, Kaur M, Yaeger D, et al. Mutations in cohesin complex members SMC3 and SMC1A cause a mild variant of Cornelia de Lange syndrome with predominant mental retardation. *Am J Hum Genet*. 2007;80:485–94.
- Deardorff MA, Wilde JJ, Albrecht M, et al. RAD21 mutations cause a human cohesinopathy. *Am J Hum Genet*. 2012;90:1014–27.
- Musio A, Selicorni A, Focarelli ML, et al. X-linked Cornelia de Lange syndrome owing to SMC1L1 mutations. *Nat Genet*. 2006;38:528–30.
- Deardorff MA, Noon SE, Krantz ID. Cornelia de Lange syndrome. In: Adam MP, Ardinger HH, Pagon RA, et al., eds. *GeneReviews*. Seattle, WA: University of Washington; 2005.
- Mannini L, Cucco F, Quarantotti V, et al. Mutation spectrum and genotype-phenotype correlation in Cornelia de Lange syndrome. *Hum Mutat*. 2013;34:1589–96.
- Lehalle D, Mosca-Boidron AL, Begtrup A, et al. STAG1 mutations cause a novel cohesinopathy characterised by unspecific syndromic intellectual disability. *J. Med. Genet*. 2017;54:479–88.
- Mullegama SV, Klein SD, Mulatinho MV, et al. De novo loss-of-function variants in STAG2 are associated with developmental delay, microcephaly, and congenital anomalies. *Am J Med Genet A*. 2017;173:1319–27.
- Soardi FC, Machado-Silva A, Linhares ND, et al. Familial STAG2 germline mutation defines a new human cohesinopathy. *NPJ Genom Med*. 2017;2:7.
- Yang Y, Muzny DM, Reid JG, et al. Clinical whole-exome sequencing for the diagnosis of mendelian disorders. *N Engl J Med*. 2013;369:1502–11.
- Yang Y, Muzny DM, Xia F, et al. Molecular findings among patients referred for clinical whole-exome sequencing. *JAMA*. 2014;312:1870–9.
- Richards S, Aziz N, Bale S, et al. Standards and guidelines for the interpretation of sequence variants: a joint consensus recommendation

- of the American College of Medical Genetics and Genomics and the Association for Molecular Pathology. *Genet Med*. 2015;17:405–24.
19. Ansari M, Poke G, Ferry Q, et al. Genetic heterogeneity in Cornelia de Lange syndrome (CdLS) and CdLS-like phenotypes with observed and predicted levels of mosaicism. *J Med Genet*. 2014;51:659–68.
 20. Gambin T, Yuan B, Bi W, et al. Identification of novel candidate disease genes from de novo exonic copy number variants. *Genome Med*. 2017;9:83.
 21. Allen RC, Zoghbi HY, Moseley AB, et al. Methylation of HpaII and HhaI sites near the polymorphic CAG repeat in the human androgen-receptor gene correlates with X chromosome inactivation. *Am J Hum Genet*. 1992;51:1229–39.
 22. Lek M, Karczewski KJ, Minikel EV, et al. Analysis of protein-coding genetic variation in 60,706 humans. *Nature*. 2016;536:285–91.
 23. Posey JE, Harel T, Liu P, et al. Resolution of disease phenotypes resulting from multilocus genomic variation. *N Engl J Med*. 2017;376:21–31.
 24. Pehlivan D, Erdin S, Carvalho CMB, et al. Evidence implicating cohesin/condensin gene noncoding CNVs in the Cornelia de Lange. (Meeting abstract) *Genomic Disorders 2012: The Genomics of Rare Diseases*. 2012.
 25. Firth HV, Richards SM, Bevan AP, et al. DECIPHER: Database of Chromosomal Imbalance and Phenotype in Humans using Ensembl Resources. *Am J Hum Genet*. 2009;84:524–33.
 26. Kline AD, Krantz ID, Sommer A, et al. Cornelia de Lange syndrome: clinical review, diagnostic and scoring systems, and anticipatory guidance. *Am J Med Genet A*. 2007;143A:1287–96.
 27. Solomon DA, Kim JS, Bondaruk J, et al. Frequent truncating mutations of STAG2 in bladder cancer. *Nat Genet*. 2013;45:1428–30.
 28. Solomon DA, Kim T, Diaz-Martinez LA, et al. Mutational inactivation of STAG2 causes aneuploidy in human cancer. *Science*. 2011;333:1039–43.
 29. Sofueva S, Yaffe E, Chan WC, et al. Cohesin-mediated interactions organize chromosomal domain architecture. *EMBO J*. 2013;32:3119–29.
 30. Kagey MH, Newman JJ, Bilodeau S, et al. Mediator and cohesin connect gene expression and chromatin architecture. *Nature*. 2010;467:430–5.
 31. Rubio ED, Reiss DJ, Welch PL, et al. CTCF physically links cohesin to chromatin. *Proc Natl Acad Sci U S A*. 2008;105:8309–14.
 32. Allen BL, Taatjes DJ. The Mediator complex: a central integrator of transcription. *Nat Rev Mol Cell Biol*. 2015;16:155–66.
 33. Strubbe G, Popp C, Schmidt A, et al. Polycomb purification by in vivo biotinylation tagging reveals cohesin and Trithorax group proteins as interaction partners. *Proc Natl Acad Sci U S A*. 2011;108:5572–7.
 34. Izumi K, Nakato R, Zhang Z, et al. Germline gain-of-function mutations in AFF4 cause a developmental syndrome functionally linking the super elongation complex and cohesin. *Nat Genet*. 2015;47:338–44.
 35. O'Rawe JA, Wu Y, Dorfel MJ, et al. TAF1 variants are associated with dysmorphic features, intellectual disability, and neurological manifestations. *Am J Hum Genet*. 2015;97:922–32.
 36. Parenti I, Gervasini C, Pozojevic J, et al. Broadening of cohesinopathies: exome sequencing identifies mutations in ANKRD11 in two patients with Cornelia de Lange-overlapping phenotype. *Clin Genet*. 2016;89:74–81.
 37. Kumar R, Corbett MA, Van Bon BW, et al. Increased STAG2 dosage defines a novel cohesinopathy with intellectual disability and behavioral problems. *Hum Mol Genet*. 2015;24:7171–81.
 38. Gillis LA, McCallum J, Kaur M, et al. NIPBL mutational analysis in 120 individuals with Cornelia de Lange syndrome and evaluation of genotype-phenotype correlations. *Am J Hum Genet*. 2004;75:610–23.
 39. Liu J, Feldman R, Zhang Z, et al. SMC1A expression and mechanism of pathogenicity in probands with X-linked Cornelia de Lange syndrome. *Hum Mutat*. 2009;30:1535–42.
 40. Goldstein JH, Tim-Aroon T, Shieh J, et al. Novel SMC1A frameshift mutations in children with developmental delay and epilepsy. *Eur J Med Genet*. 2015;58:562–8.

¹Department of Molecular and Human Genetics, Baylor College of Medicine, Houston, Texas 77030, USA. ²Baylor Genetics, Houston, Texas 77021, USA. ³Texas Children's Hospital, Houston, Texas 77030, USA. ⁴Department of Pediatrics, Section of Child Neurology, Baylor College of Medicine, Houston, Texas 77030, USA. ⁵Seattle Children's Hospital, Seattle, Washington 98105, USA. ⁶Department of Pediatrics, University of Washington School of Medicine, Seattle, Washington 98105, USA. ⁷University of Exeter Medical School, RILD Wellcome Wolfson Centre, Royal Devon & Exeter NHS Foundation Trust, Barrack Road, Exeter EX2 5DW, UK. ⁸Peninsula Clinical Genetics Service, Royal Devon & Exeter Hospital, Gladstone Road, Exeter EX1 2ED, UK. ⁹Clinical Genetics Service, NHS Grampian, Aberdeen AB25 2ZA, Scotland. ¹⁰Department of Pediatrics, University of Rochester Medical Center, Rochester, New York 14642, USA. ¹¹Department of Pediatrics, Nationwide Children's Hospital, Columbus, Ohio 43205, USA. ¹²Division of Medical Genetics, Stanford University, Stanford, California 94305, USA. ¹³Rare Disease Institute, Children's National Health System, Washington, DC 20010, USA. ¹⁴Children's Hospital of Pittsburgh of UPMC, Pittsburgh, Pennsylvania 15224, USA. ¹⁵Department of Medical Genetics, Oslo University Hospital, 0424 Oslo, Norway. ¹⁶Norwegian National Unit for Newborn Screening, Division of Pediatric and Adolescent Medicine, Oslo University Hospital, 0424 Oslo, Norway. ¹⁷Department of Medical Genetics, Telemark Hospital Trust, 3710 Skien, Norway. ¹⁸New Leaf Center, Clinic for Special Children, Mt. Eaton, Ohio 44659, USA. ¹⁹Division of Genetics and Genomic Medicine, Department of Pediatrics, Washington University School of Medicine, St. Louis, Missouri 63110, USA. ²⁰Dell Children's Medical Center of Central Texas, Austin, Texas 78723, USA. ²¹Institute of Human Genetics, University Hospital Cologne, Cologne, Germany. ²²Center for Molecular Medicine Cologne, University of Cologne, Cologne, Germany. ²³Center for Rare Diseases, University Hospital Cologne, Cologne, Germany. ²⁴Center for Human Genetics, Department of Human Genetics, KU Leuven, 3000 Leuven, Belgium. ²⁵Department of Pediatrics, Baylor College of Medicine, Houston, Texas 77030, USA. ²⁶Department of Human Genetics, Emory University, Atlanta, Georgia 30322, USA